Cancer Chemotherapy and Pharmacology (2019) 83:81–89
https://doi.org/10.1007/s00280-018-3705-6

ORIGINAL ARTICLE

Plasma and brain pharmacokinetics of letrozole and drug interaction studies with temozolomide in NOD-*scid* gamma mice and sprague dawley rats

Priyanka Arora[1] · Courtney Huff Adams[1] · Gary Gudelsky[1] · Biplab DasGupta[2] · Pankaj B. Desai[1]

Received: 17 July 2018 / Accepted: 15 October 2018 / Published online: 24 October 2018

Abstract

Purpose The aromatase inhibitor, letrozole, is being investigated in experimental animal models as a novel treatment for high-grade gliomas (HGGs). To facilitate optimal dosing for such studies, we evaluated the plasma and brain pharmacokinetics (PK) of letrozole in NOD-scid gamma (NSG) mice, which are frequently employed for assessing efficacy against patient-derived tumor cells. Furthermore, we evaluated the potential PK interactions between letrozole and temozolomide (TMZ) in Sprague–Dawley rats.

Methods NSG mice were administered letrozole (8 mg/kg; i.p) as a single or multiple dose (b.i.d, 10 days). Brain tissue and blood samples were collected over 24 h. Letrozole and TMZ interaction study employed jugular vein-cannulated rats (three groups; TMZ alone, letrozole alone and TMZ + letrozole). Intracerebral microdialysis was performed for brain extracellular fluid (ECF) collection simultaneously with venous blood sampling. Drug levels were measured employing HPLC and PK analysis was conducted using Phoenix WinNonlin®.

Results In NSG mice, peak plasma and brain tissue letrozole concentrations (C_{max}) were 3–4 and 0.8–0.9 µg/ml, respectively. The elimination half-life was 2.6 h with minimal accumulation following multiple dosing. In the drug interaction study, no PK changes were evident when TMZ and letrozole were given in combination. For instance, peak plasma and brain ECF TMZ levels when given alone were 14.7 ± 1.1 and 4.6 ± 0.6 µg/ml, respectively, and 12.6 ± 2.4 and 3.4 ± 0.8 µg/ml, respectively, when given with letrozole.

Conclusions These results will guide the optimization of dosing regimen for further development of letrozole for HGG treatment.

Keywords Drug–drug interactions · Blood brain barrier · Letrozole · Temozolomide · Pharmacokinetics

Introduction

Treatment of primary brain tumors remains one of the most formidable challenges in oncology.

According to the Central Brain Tumor Registry of the United States (CBTRUS), 19,000 primary malignant HGGs will be diagnosed in 2018 [1, 2]. The overall prevalence of HGGs is about 111,000, and, as such, this malignancy is considered as an orphan disease. The standard of care for HGGs, which unfortunately has not changed significantly over the past decade, includes maximal safe tumor resection upon diagnosis, followed by adjuvant radiation and chemotherapy with TMZ [3, 4]. Due to the invasive nature of this disease that often leads to spread within the CNS and the inherent chemoresistance of the tumor cells, most patients experience recurrence or progression of their disease. Unfortunately, the disease recurs in almost all patients with few, if any, therapeutic options available thereafter [3, 5]. Consequently, the prognosis for patients with HGG remains dismal. For instance, glioblastoma multiforme (GBM, grade IV astrocytoma), which is one of the most aggressive and treatment-resistant tumors and accounts for over half of all gliomas, is associated with a median survival of 14.6 months

✉ Pankaj B. Desai
desaipb@ucmail.uc.edu

[1] Division of Pharmaceutical Sciences, College of Pharmacy, James L. Winkle College of Pharmacy, University of Cincinnati, 231 Albert Sabin Way, Cincinnati, OH 45267, USA

[2] Division of Oncology, Cincinnati Children's Hospital Medical Center, Cincinnati, OH, USA

[4]. Major limitations of chemotherapy for gliomas include inability of many drugs to adequately cross the blood–brain/blood-tumor barrier, and lack of validated targets for novel treatments [6–8].

Recent studies suggest that the enzyme aromatase (CYP19A1), also known as estrogen synthetase, a well-known target for the treatment of estrogen receptor (ER) positive breast cancer [9], may also be an attractive novel target for the treatment of HGGs. In ongoing immunohistochemical analyses of patient-derived tumor samples, we observed that the expression of aromatase is markedly higher in HGGs than that in normal brain tissue and low-grade gliomas [10]. In addition, Duenas Jimenez et al. (2014) analyzed aromatase and ERα and ERβ expression in biopsy samples from 36 patients with grade I–IV astrocytoma [11]. Aromatase expression (CYP19A1 mRNA) and estradiol levels in tumor tissues were reported as significantly higher in grade III/IV astrocytomas relative to grade II astrocytoma and directly correlated with tumor grade. Second, our PK studies performed in rats orthotopically implanted with rat C6 gliomas revealed that the aromatase inhibitor letrozole easily penetrates the blood–brain barrier (BBB), with intratumoral levels 1.5-2-fold higher relative to normal brain tissue [12]. Pharmacodynamic studies conducted employing micro-PET/CT imaging showed that daily treatment with letrozole resulted in > 80% shrinkage of tumors with a 15 day treatment course [13]. Recently, Tivnan et al. (2017) assessed aromatase expression in several primary and recurrent patient-derived GBM cells in vitro [14]. Western blot analysis indicated that protein lysates from all of these cells expressed significant levels of aromatase and that letrozole markedly inhibited cell proliferation and migration and reduced spheroid formation. Thus, it appears that letrozole may have an important role in the treatment and management of HGGs.

To gain further clinical insights of our studies thus far, here we first conducted letrozole PK studies in NSG immunocompromised mice frequently used in the studies with patient-derived tumor xenografts [15–17]. Furthermore, given that TMZ is the current standard of care, any new agent for treating HGGs needs to be investigated in combination with this agent. Thus, we assessed the potential for PK drug–drug interactions between letrozole and TMZ and examined if co-administration affected plasma and brain PK of these agents.

Materials and methods

Chemicals and supplies

Letrozole and TMZ were purchased from Toronto Research Chemicals (Toronto, Canada). Letrozole solution for intra-peritoneal administration was prepared in bacteriostatic normal saline solution (Braun Medical Inc., Bethlehem, PA) containing 10% Tween-20 (VWR Scientific, Philadelphia, PA) while TMZ was prepared in water for injection (Thermo Fisher Scientific, Waltham, MA). Theophylline (internal standard, for TMZ analysis) was obtained from Sigma-Aldrich (St. Louis, MO). Ethyl acetate, methyl tertiary butyl ether, methanol, acetic acid and acetonitrile of HPLC grade were purchased from Fisher Scientific (Hanover Park, IL, USA) and the heparin-dextrose lock solution was obtained from Sai Infusion Technologies (Lake Villa, IL). Other reagents were of analytical grade and were purchased from Fisher Scientific (Hanover Park, IL). Microdialysis membrane with an outside diameter of 216 µm and a molecular weight cut-off of 13 kDa was obtained from Spectrum laboratories (Rancho Dominguez, CA) and K2-EDTA coated tubes were purchased from VWR Scientific (Philadelphia, PA).

Animals

Adult female jugular vein cannulated Sprague–Dawley rats (age, 9–11 weeks; weight, 200–225 g) (Charles River Laboratories) and female NSG mice (age, 10 weeks; weight, 20–25 g) were used for this study. All the experiments were conducted in strict accordance with the Institutional Animal Care and Use Committee (IACUC)-approved protocols of Cincinnati Children's Hospital Medical Center (CCHMC) and University of Cincinnati and the study was compliant with all the relevant ethical guidelines of animal research. Upon arrival, animals were housed under pathogen-free, temperature and humidity-controlled environment on a 12/12 h light/dark cycle and were given access to standard chow and water ad libitum. To maintain the patency of the jugular vein catheters, they were flushed with normal saline and heparin-dextrose solution every other day.

PK study of letrozole in NSG mice

Brain and plasma PK of letrozole were assessed in NSG mice ($N = 48$). Brain tissue and blood/plasma samples were collected at eight different time points (0, 0.5, 1, 2, 4, 8, 12, and 24 h) following administration of letrozole at a single dose of 8 mg/kg IP or 8 mg/kg IP, bid for 10 days. At the designated time points, mice were decapitated to remove the brain tissue, followed by trunk blood collection. Harvested tissues were carefully washed with deionized water and frozen using dry ice while the blood samples were collected in EDTA coated collection vials and centrifuged at 4000 rpm for 15 min to separate plasma. Both brain and plasma samples were stored at − 80 °C until analyzed.

PK studies of TMZ and letrozole in Sprague–Dawley Rats

The plasma and brain ECF microdialysis studies were done as described earlier [12, 18].

Construction of microdialysis probes

Concentric-style microdialysis probes with an outer diameter of 210 µm and an active length of 4.5 mm were constructed with hollow fiber membrane (molecular weight cut off, 13 kDa). The inlet tubing was PE-20 (0.38 mm I.D., 1.09 mm O.D., 8 cm long, Becton Dickinson, Sparks, MD) and the outlet tubing was fused silica (75 µm I.D., 147 µm O.D., 5 cm long, Polymicro Technologies, Phoenix, AZ) within Tygon tubing (21 cm long, Fischer Scientific). Probe components were affixed to 26G hypodermic tubing (0.01″ I.D., 0.018″ O.D., 19 mm long) using epoxy. The average in vitro relative recovery of TMZ was 12.4% at a flow rate of 2.0 µl/min at 35 °C.

Microdialysis surgery

Microdialysis probes were surgically implanted in jugular vein cannulated rats under anesthesia (ketamine/xylazine 70/ 6 mg/kg i.p., Henry Schein, NY) one day prior to the experiment. Buprenorphine (Buprenex®, Henry Schein, NY) was administered for perioperative analgesia. The probe was inserted into the striatum with the following tip coordinates: A/P, 1.2 mm, L, 3.1 mm, and D/V −7.8 mm, according to the stereotaxic atlas of Paxinos and Watson [19]. The active portion of the membrane for the probes was 4.5 mm. Following implantation, the probes were connected to an infusion pump set to deliver modified Dulbecco's phosphate buffered saline containing 1.2 mm $CaCl_2$ and 5 mM glucose at a flow rate of 1 µl/min overnight. On the day of microdialysis, the flow rate was increased to 2 µl/min and the probes were allowed to equilibrate for 2 h before sample collection.

Drug administration and blood/brain ECF sample collection

Following probe equilibration, rats were divided into three groups ($N=9$; 3/ group). Group 1: TMZ, 20 mg/kg IP; group 2: letrozole, 4 mg/kg IP; and group 3: TMZ 20 mg/kg + letrozole 4 mg/kg. Blood samples were collected in K2- EDTA coated tubes through the jugular vein catheters at the following time points- pre-dose, 0.25, 0.5, 0.75, 1, 2, 3, 4, 6 and 8 h post drug administration. Within 10 min of collection, plasma was separated by centrifugation of the blood samples at 4,000 rpm for 15 min. To chemically stabilize TMZ, plasma samples from the TMZ alone and TMZ + letrozole groups were placed in Eppendorf tubes containing 0.01 ml of 8.5% phosphoric acid to adjust the pH at 4. Microdialysis samples were collected simultaneously through the probes at the same time points from 0 to 8 h. For letrozole alone and the combination group, blood sample collection was continued up to 72 h to evaluate the bidirectional effect of TMZ on letrozole plasma PK. All the samples were stored at − 80 °C until analysis.

HPLC analysis of TMZ and letrozole

Sample preparation

Letrozole was extracted from plasma and brain tissue samples using the liquid–liquid extraction technique. Excised whole brain tissue was homogenized with two parts of normal saline. Samples for generating calibration curves were prepared by spiking pooled blank plasma or brain tissue from untreated mice with known letrozole concentrations to yield 9–10 samples ranging from 5 to 5000 ng/ml. A 50 µl aliquot of the plasma/ brain homogenate was transferred to a glass tube containing 1 mL of the extraction solvent methyl-tertiary-butyl ether. All samples were vortex mixed for 40 s and centrifuged for 5 min and 800 µl of the supernatant was decanted into a clean test tube and evaporated to dryness using a CentriVap evaporator. The residue was reconstituted with 100 µl mobile phase and 50 µl of sample volume was injected onto the HPLC system for analysis.

Liquid–liquid extraction was also employed for TMZ analysis from the plasma samples. Calibration standards were freshly prepared by spiking working TMZ solution into the blank rat plasma to give a concentration curve ranging from 50 to 20,000 ng/mL. Briefly, 50 µl of the acidified plasma/ standard was transferred to a glass tube containing 500 ng/ml of the internal standard, theophylline, followed by addition of 1 ml of the extraction solvent ethyl acetate. All the samples were then extracted using the aforementioned method. The dialysis samples, on the other hand, were injected directly onto HPLC.

Chromatographic condition

We employed a modified published method for TMZ HPLC analysis [20]. Briefly, the analysis was conducted under ambient conditions with a Waters HPLC system using a reversed phase Waters XTerra C18 column (150 × 4.6 mm, particle size of 5 µm) and a Waters dual absorbance UV detector. The UV wavelengths were set at $\lambda = 330$ nm for TMZ and $\lambda = 276$ nm for the internal standard. Mixture of 0.5% acetic acid/ methanol (80:20, v/v) was used as the mobile phase at a flow rate of 1.0 mL/min employing an isocratic elution mode. TMZ and the internal standard peaks had a retention time of 2.7 and 4.6 min, respectively. Three sets of calibration curves, where known TMZ concentrations ranged from 10 to 20,000 ng/ml, were constructed for

method validation. These standard curves were linear over this concentration range, with the lower limit of detection of 10 ng/ml and a relative standard deviation (RSD) varying between 1.2 and 3.7%.

For chromatographic analysis of letrozole, Waters HPLC system comprising a reversed phase Waters BDS Hypersil C18 column (100 × 4.6 mm, particle size of 5 µm) and a Waters scanning fluorescence detector (Model 474) with excitation and emission wavelengths of 230 and 295 nm, respectively, were used [12]. Phosphate buffer/ acetonitrile (65:35, v/v; pH 10.2) delivered at a flow rate of 1.0 ml/min was employed as the mobile phase. Letrozole peaks were detected at a retention time of around 2.6 min. Again, three sets of calibration curves where known letrozole concentrations ranged from 5 to 5,000 ng/ml were constructed for method validation. These standard curves were linear over this concentration range, with the lower limit of detection of 5 ng/ml and a relative standard deviation (RSD) varying between 0.7 and 3.9%.

PK data analysis

Non-compartmental analysis was performed using Phoenix WinNonlin software (version 6.2.1, Pharsight, St. Louis, MO, USA) and the PK parameters determined included peak concentration (C_{max}), time to reach peak concentration (T_{max}), area under the concentration–time curve between time zero, the last observed concentration time point (AUC_{0-t}) and the elimination half-life ($t_{1/2}$). Actual sampling times were employed for calculations except for the pre-dose times, which were kept as zero. AUC_{0-t} was calculated using the linear trapezoidal method and $C_{max\ and}$ T_{max} values were obtained directly from the concentration–time data. The overall elimination rate constant (K_{10}) was determined from the best fitting non-linear regression curve of the terminal portion of the concentration–time profile and the elimination half-life $t_{1/2} = \ln(2)/k_{10}$. Brain ECF concentrations were time-averaged over the collection interval and were corrected for the observed relative recovery.

The brain-to-plasma partition coefficients (K_{puu}) of TMZ were calculated as a ratio of the C_{max} or AUC of TMZ concentration in the brain ECF to corresponding plasma C_{max} and AUC values corrected for unbound fraction of the drug in plasma. Based on previous publications, the unbound fraction of TMZ is about 85% [21].

Statistical analysis

Key PK parameters were evaluated for statistical differences using the Analysis of Variance (ANOVA) method followed by two-tailed *t* test. All data were expressed as the mean ± standard deviation (SD). Differences were considered statistically significant at p value < 0.05.

Results

Single dose and steady state letrozole PK studies in NSG mice

We evaluated both plasma and brain tissue letrozole PK following single and multiple doses of 8 mg/kg given by the i.p. route. For multiple dosing letrozole was administered twice daily for 10 days to ensure that steady state was reached. Blood and tissue samples were collected over a 24 h-period after last dose administration. Single versus multiple dose plasma and brain tissue concentration–time profiles of letrozole are shown in Fig. 1a, b, respectively. The PK parameters are summarized in Table 1. Letrozole brain penetration across the blood–brain barrier was relatively rapid as apparent by the short T_{max} of 2 h. The plasma and brain tissue elimination half-lives were 2.8 and 2.7 h, respectively. Based on these relatively short half-lives, a 10-day period was adequate to ascertain that steady state was achieved. The peak plasma and brain tissue levels after single dose and at

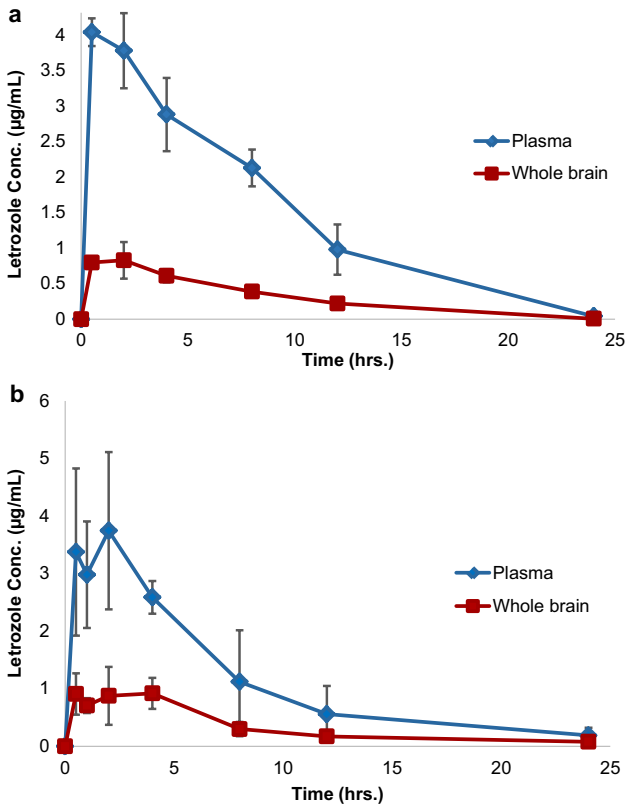

Fig. 1 Letrozole plasma and brain tissue PK in NSG mice. Letrozole was administered via the intraperitoneal route at a single dose of 8 mg/kg (**a**) or 8 mg/kg bid for 10 days (**b**). Trunk blood and brain tissue samples were collected at the indicated time points from 0 to 24 h. Data; mean ± SD ($N = 3$ mice/time point); concentration of letrozole in plasma (filled diamond) and brain (filled square)

Table 1 Single dose and steady state PK parameter estimates of letrozole in plasma and brain tissue in NSG mice

PK parameter	Plasma	Brain	Kp_{brain} [a]
N	24	24	
T_{max} (h)			
Day 1	0.5	2.0	–
Day 11	2.0	4.0	–
Half-life $t_{1/2}$ (h)			
Day 1	2.8	2.7	–
Day 11	6.5	6.3	–
C_{max} (µg/ml)			
Day 1	4.0	0.8	0.2
Day 11	3.8	0.9	0.2
AUC_{0-24} (h µg/ml)			
Day 1	35.9	7.5	0.2
Day 11	27.5	8.1	0.3
$AUC_{0-\infty}$ (h µg/ml)			
Day 1	36.2	7.6	0.2
Day 11	29.2	9.0	0.3
R (AUC_{0-24} ratio of Day 11/Day 1)	0.8	1.1	–

[a]The brain-to-plasma partition coefficient (Kp_{brain}) was determined as the ratio of the total brain tissue C_{max} or AUC with corresponding values in plasma

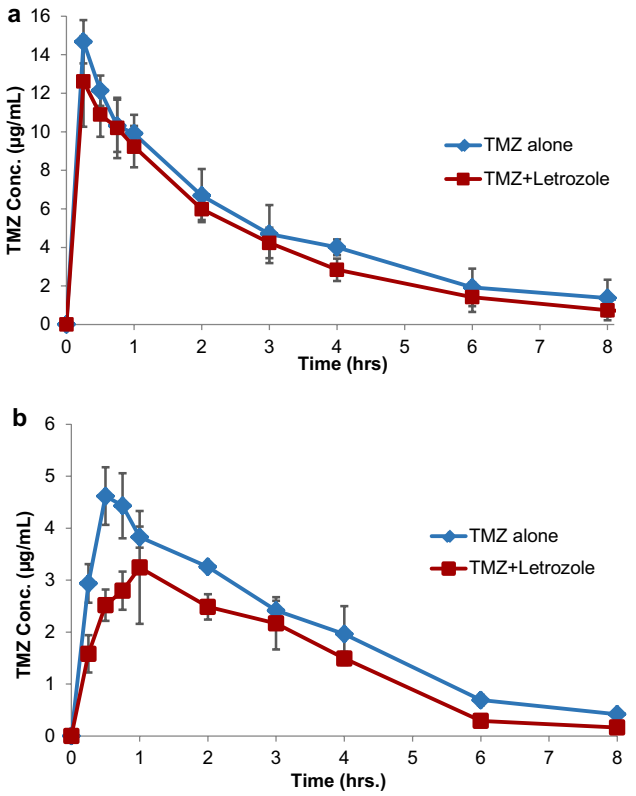

Fig. 2 Plasma and brain ECF PK of TMZ with or without co-administration of letrozole in Sprague Dawley rats. A single dose of TMZ (20 mg/kg, i.p.) was administered to rats either alone or in combination with letrozole (4 mg/kg, i.p.). Plasma samples were collected through the jugular vein catheters and brain ECF samples were collected employing intracerebral microdialysis. Blood and microdialysate samples were collected at discrete time intervals from 0 to 8 h. Plasma concentration–time profiles of TMZ with or without letrozole (**a**) and brain ECF concentration–time profiles of TMZ with or without letrozole (**b**). Data; mean ± SD; *N* = 3 rats/treatment group. (filled diamond; TMZ alone) and (filled square; TMZ + Letrozole)

steady state were 4.0 and 0.8 µg/ml and 3.8 and 0.9 µg/ml, respectively. These data suggest that there was no accumulation of the drug with b.i.d. dosing and the brain tissue/plasma partitioning ratios ranged from 0.2 to 0.3.

Plasma and Brain ECF PK Studies on TMZ and letrozole

For the drug interaction study, we employed jugular vein cannulated rats and intracerebral microdialysis to facilitate simultaneous serial plasma and brain ECF sampling in individual rats. Figure 2 depicts the plasma and brain ECF PK profiles of TMZ with or without co-administration of letrozole. Based on previous publications that document a TMZ elimination half-life of 1–2 h [21, 22], blood and ECF samples were collected over an 8-h period. The brain ECF concentrations were corrected for a recovery factor of 12.4%. As shown in Table 2, there were no statistically significant differences in time to peak, elimination half-life and systemic exposure (C_{max} and AUC) of TMZ in both brain ECF and plasma. There was considerable variability in the brain ECF PK of TMZ. While there was an increase in the T_{max} and a reduced AUC in the brain ECF, these differences were also deemed to be statistically insignificant. When corrected for plasma protein binding of TMZ (~ 85%), the brain-to-plasma (unbound fraction) partition coefficient (K_{puu}) ranged from 0.3 to 0.5 on the basis of C_{max} or AUC ratios as shown in Table 2.

The plasma concentration–time profiles of letrozole with and without TMZ are shown in Fig. 3. Based on our previous studies that delineated brain penetration of letrozole in this animal model, brain ECF measurements were not performed here. In addition, based on the letrozole plasma half-life in female Sprague Dawley rats of approximately 40 h [23], we collected blood samples for a period of 72 h. As shown in Table 3, TMZ administration had little impact on the plasma PK of letrozole with no statistically significant changes noted in the elimination half-live and systemic exposure based on C_{max} and AUC values.

Table 2 Brain ECF and plasma PK of TMZ in rats following intraperitoneal administration of TMZ alone or in combination with letrozole

PK parameter	Brain ECF	Plasma	K_{puu} [a]
TMZ alone			
N	3	3	
T_{max} (h)	0.5 ± 0.00	0.3 ± 0.00	–
Half-life $t_{1/2}$ (h)	2.0 ± 0.1	2.4 ± 1.0	–
C_{max} (μg/ml)	4.6 ± 0.6	14.7 ± 1.1	0.37 ± 0.02
AUC_{0-8} (h μg/ml)	15.8 ± 1.2	38.1 ± 6.1	0.46 ± 0.03
$AUC_{0-\infty}$ (h μg/ml)	17.0 ± 1.1	43.9 ± 9.3	0.46 ± 0.03
TMZ + Letrozole			
N	3	3	
T_{max} (h)	1.3 ± 0.5 (0.225*)	0.3 ± 0.00	–
Half-life $t_{1/2}$ (h)	1.3 ± 0.3 (0.119*)	1.8 ± 0.7 (0.267*)	–
C_{max} (μg/ml)	3.4 ± 0.8 (0.210*)	12.6 ± 2.4 (0.243*)	0.33 ± 0.05
AUC_{0-8} (h μg/ml)	12.3 ± 1.1 (0.051*)	32.3 ± 4.8 (0.331*)	0.43 ± 0.09
$AUC_{0-\infty}$ (h μg/ml)	15.0 ± 1.2 (0.052*)	35.5 ± 6.4 (0.338*)	0.49 ± 0.09

Data represented as mean ± SD. Dialysate concentrations were corrected for in vitro recovery of TMZ (estimated to be 12.4%)

$p > 0.05$ suggests NO significant difference based on the two-tailed *t* test

*Represents the *p* values calculated for the PK parameter estimates from the combination group in comparison with the TMZ alone group

[a]K_{puu} unbound partition coefficient in brain, measured as the ratio of C_{max} or AUC of TMZ in brain ECF to the corresponding values in plasma when corrected for protein binding. Fraction unbound for TMZ in plasma is 0.85

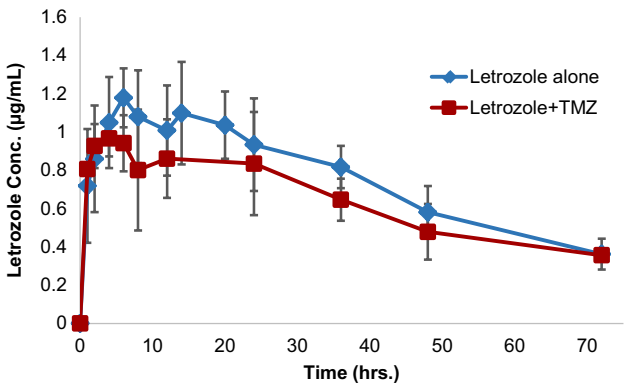

Fig. 3 Plasma PK of letrozole in Sprague–Dawley rats when given alone and in combination with TMZ. Following single dose administration of letrozole (4 mg/kg) with or without TMZ (20 mg/kg) via the intraperitoneal route, plasma samples were collected up to 72 h. Data; mean ± SD; *N* = 3 rats/treatment group. (filled diamond; Letrozole alone) and (filled square; Letrozole + TMZ)

Table 3 Plasma PK of letrozole alone or when co-administered with TMZ in rats

PK parameter	Letrozole alone	Letrozole + TMZ	*p* value
Plasma			
N	3	3	
T_{max} (h)	8.5 ± 4.6	4.0 ± N.A	
Half-life $t_{1/2}$ (h)	34.0 ± 3.2	39.1 ± N.A	–
C_{max} (μg/ml)	1.2 ± 0.1	1.0 ± 0.1	0.127
AUC_{0-72} (h μg/ml)	54.4 ± 11.3	45.9 ± 12.0	0.384

Data represented as mean ± SD

N.A. not available

$p > 0.05$ suggests NO significant difference based on the two-tailed *t* test

Discussion

Novel therapeutics for targeting aggressive malignancies with dismal prognosis such as HGGs are urgently needed. Based on recent findings that the expression of the monooxygenase, aromatase (CYP19A1), is markedly higher in HGGs, this enzyme appears to be a promising new target. Aromatase catalyzes the conversion of androgens to estrogens in peripheral tissues and is a well-known target for the treatment of estrogen receptor positive breast cancer in post-menopausal women. Indeed, the use of aromatase inhibitors has become the mainstay for the treatment of ER positive breast cancer in the post-menopausal women. In that regard, one of the most extensively used aromatase inhibitor with well-documented record of efficacy and safety is letrozole [24, 25]. Thus, the discovery of selectively high expression of aromatase provides an opportunity for investigation of the potential use of letrozole as a new therapeutic agent for HGGs [10–14]. Accordingly, our initial studies have documented that letrozole has robust penetration across the BBB and marked anti-tumor efficacy in Sprague Dawley rats orthotopically implanted with C6 glioma, a commonly used experimental model for HGGs [12]. Here, we extended the PK studies to gain additional clinical insights.

We first assessed single dose and steady state PK of letrozole in NSG mice, an immunocompromised mouse model, which is a commonly employed preclinical animal model in oncology research to assess anti-tumor efficacy of investigational agents against patient-derived tumor cells [15–17]. In contrast to the previously reported half-life of letrozole of approximately 40 h in female rats [23, 26] which was corroborated in this study, the half-life in female NSG mice was less than 3 h. Not surprisingly, with twice daily dosing there was no accumulation and the steady state plasma and brain tissue levels of letrozole were similar to those observed with a single dose administration. Our observation that the elimination half-life of letrozole is much shorter in mice

relative to other species is consistent with previous reports [27]. However, reasons for this are not clear. In humans, letrozole is largely eliminated via hepatic metabolism mediated primarily by cytochrome P450 CYP2A6 with a minor contribution of CYP3A4 [28]. In mice, there is considerable inter-strain variation in the expression of CYP2A5, mouse orthologous of human CYP2A6, with strains such as DBA-1 and DBA-2 having markedly higher constitutive expression [29]. While data for letrozole metabolism in NSG mouse liver tissue are not available, we conjecture that the hepatic intrinsic clearance of this drug is relatively high resulting in much shorter elimination half-life.

Unlike our studies in rats, intracerebral microdialysis in mice has significant technical difficulties including inability to collect sufficient ECF to facilitate bioanalysis. Moreover, since only a small volume of blood can be collected from each mouse, the blood sampling procedure necessitated terminating the animal at the time of blood sample collection via cardiac puncture. Thus, we opted to simultaneously collect brain tissues at the time of blood sample collection. The partitioning of the drug from blood into the brain, as gleaned from the brain/plasma ratio (Kp), was determined using both the peak plasma concentrations as well as the AUC. The overall brain partitioning of letrozole ranged from 0.2 to 0.3 in mice. This is in good agreement with the previously reported value of 0.38 in male wild-type ICR mice by Miyajima et al. (2013) [6]. In our studies with Sprague–Dawley rats, the ratio of letrozole in brain tissue/brain ECF is approximately 1.5 (data not shown). Assuming that ratio is similar in NSG mice and with the reported plasma protein binding of 60%, the projected brain ECF/plasma$_{ub}$ can be estimated to be about 0.3. Relative to the well-known inability of most xenobiotics to cross the BBB, this ratio is suggestive of adequate CNS exposure of the drug. However, this is considerably lower than the brain ECF/plasma$_{ub}$ ratio of approximately 0.5 to 1.0 [12] that we observed in the rats. Therefore, based on the short half-life and lower brain tissue concentrations, the dosing regimen of letrozole in NSG mice may necessitate potentially more frequent drug administration, perhaps 3–4 times/day, and/or doses higher than those employed in our efficacy studies in Sprague–Dawley rats [13]. The efficacy studies will have to be carefully balanced against potential toxicity of the drug. During the multiple dosing study, we did observe signs of overt toxicity such as weight loss and we may have to opt for using alternative mouse strain or immunocompromised rats for studies against patient-derived xenografts.

The brain to plasma partitioning ratio (K_{puu}) of TMZ in rats was determined on the basis of the observed brain ECF C_{max} or AUC relative to the corresponding unbound plasma C_{max} or AUC values. Our observed values of 0.3–0.5 are consistent with those reported earlier from pre-clinical and clinical studies. Zhou and colleagues employed intracerebral microdialysis in male athymic rats following an i.v. administration of 20 mg/kg and reported a K_{puu} value of 0.22 [30]. In the clinical setting, brain penetration insights were derived directly from intracerebral microdialysis in patients with primary or metastatic brain tumors where the AUC$_{ecf}$/AUC$_{plasma}$ was 17.9 ± 13.3% [31]. When corrected for protein binding the average ratio is estimated to be about 21%. In another study where plasma and cerebrospinal fluid sampling was performed, the (AUC$_{csf}$/AUC$_{plasma}$) ratio for TMZ ranged from 20 to 30% [32].

For the drug–drug interaction study, we preferred to employ Sprague–Dawley rats since that allows simultaneous plasma and brain ECF sampling and facilitates unbound brain ECF/plasma partitioning for each individual rat. Additionally, the elimination half-life of letrozole in rats is much longer, which is closer to that observed in humans [23, 26]. As such, any potential drug interaction may be discerned at clinically relevant plasma levels and systemic exposure of letrozole using the rat model. For TMZ, we employed a dose of 20 mg/kg. The clinical dose of TMZ is 200 mg/m^2 and based on the average body surface areas, it approximately translates to a dose of 20–30 mg/kg in rats [22] and the dose of 20 mg/kg we employed here has been frequently used in pre-clinical studies [30]. While for letrozole, we continued the use of a dose of 4 mg/kg as that was noted to be effective against orthotopically implanted C6 glioma in Sprague–Dawley rats in our previous study [13]. The co-administration of letrozole did not impact the plasma or brain elimination half-lives, peak levels and AUC of TMZ. At a systemic level, these two agents do not share clearance pathways. TMZ is an imidazotetrazine which is completely bioavailable after per oral administration ($F = 100\%$) and has an elimination half-life in human in the range of about 2 h [21, 22, 33]. At physiological pH, TMZ undergoes non-enzymatic spontaneous hydrolysis to 5-(3-methyltriazen-1-yl) imidazole-4-carboxamide (MTIC). A short-lived intermediate with an elimination half-life of 2 min, MTIC rapidly breaks down to form the reactive methyldiazonium ion that alkylates DNA, with 5-aminoimidazole-4-carboxamide (AIC) as a side product [21, 22]. AIC and other polar metabolites of TMZ are then cleared by the renal route. About 5% of unchanged TMZ is also recovered in the urine [21]. MTIC produced in plasma is not able to cross BBB and as such it is formed locally in the brain [33]. Given its short half-life, the PK of MTIC in the brain is governed by that of TMZ. Thus, determining TMZ PK is reflective of MTIC formation and clearance. Therefore, we did not measure the levels of MTIC in brain ECF.

With mutually exclusive clearance pathways, the risk for systemic drug–drug interaction between these two agents was anticipated to be low. Nevertheless, it was also important to address potential impact of letrozole administration on the BBB penetration and brain PK of TMZ. Recent

studies indicate that TMZ is a substrate of efflux transporters P-glycoprotein (P-gp) and the breast cancer resistance protein (BCRP) [34–36]. There is evidence to suggest that estrogen receptor mediated signaling impacts the activity of BCRP and P-gp at the BBB [37–40]. In rats, estradiol was shown to downregulate the expression of BCRP in the brain capillaries [37]. Accordingly, inhibition of in situ estradiol production by letrozole may potentially impact the expression of BCRP, which may result in increasing BCRP mediated efflux and lowering the brain concentrations of TMZ. Thus, it is conceivable that letrozole may impact TMZ brain concentrations without affecting its systemic clearance. However, in the present study no acute effects of letrozole on the rate and extent of TMZ penetration and PK in the brain ECF were apparent.

The co-administration of TMZ did not alter the plasma PK of letrozole. Unlike AUC_{0-inf} estimates of letrozole in mice or that of TMZ in rats, we were constrained to determining AUC_{0-72} for letrozole in rats. Since letrozole plasma half-life in rats was quite long (~ 34–40 h), a 72-h sampling period accounts for only about 75% drug elimination. Consequently, AUC_{0-inf} values could not have been reliably determined. Also, we did not assess letrozole brain ECF PK with and without TMZ administration. A technical restriction is imposed by the small volume of microdialysate fluid (~ 50 µl) available over time intervals of 30–60 min which limited analysis to only one analyte. As such, we were constrained to the quantitation of only TMZ in brain ECF. However, based on our extensive experience with letrozole neuropharmacokinetic studies [12], we postulate that a lack of observed impact of TMZ on letrozole systemic PK suggests that the overall brain exposure of letrozole is also not impacted with TMZ co-administration. Letrozole is not a substrate for efflux transport [6] and its biopharmaceutical properties and the previously observed high plasma to brain partitioning (ranging from 0.5 to 1) suggests that its BBB penetration is primarily due to passive diffusion.

In conclusion, our pre-clinical PK studies presented here extends our previously reported PK studies on letrozole and provides additional clinically relevant insights. Based on single dose and steady state PK assessments, it appears that letrozole is rapidly eliminated from NSG mice with little accumulation in plasma and brain tissue upon multiple dosing. As such, dosing regimens that sustain drug levels may have to be implemented when employing this mouse model of anti-tumor efficacy studies against HGGs. Using intracerebral microdialysis in conjunction with blood sampling, we show here that letrozole and TMZ co-administration did not exhibit pharmacokinetic drug–drug interactions. On a related note, in a sub-chronic 20 day toxicity study, no overt toxicity (body weight, lack of diet, neuromuscular toxicity and overall appearance) were observed upon daily i.p. administration of TMZ (20 mg/kg) and letrozole (4 mg/kg) in Sprague Dawley rats. Overall, with a lack of bi-directional pharmacokinetic interactions both in brain and plasma, and with the absence of acute toxicity, the combination of TMZ and letrozole may not have safety concerns.

Acknowledgements The study was supported by grants from the University of Cincinnati Brain Tumor Center Molecular Therapeutics Program, Neuroscience Institute and Technology Commercialization Accelerator.

Compliance with ethical standards

Conflict of interest All authors declare that they have no conflict of interest.

Ethical approval All the experiments were conducted in strict accordance with the Institutional Animal Care and Use Committee (IACUC)-approved protocols of Cincinnati Children's Hospital Medical Center (CCHMC) and University of Cincinnati and were performed as per the highest international standards of animal welfare outlined by the NIH's Guide for the Care and Use of Laboratory Animals.

References

1. Ostrom QT, Gittleman H, Liao P et al (2017) CBTRUS statistical report: primary brain and other central nervous system tumors diagnosed in the united states in 2010–2014. Neuro Oncol 19(suppl_5):v1–v88
2. Ostrom QT, Gittleman H, Stetson L, Virk S, Barnholtz-Sloan JS (2018) Epidemiology of intracranial gliomas. Prog Neurol Surg 30:1–11
3. Franceschi E, Minichillo S, Brandes AA (2017) Pharmacotherapy of glioblastoma: Established treatments and emerging concepts. CNS Drugs 31(8):675–684
4. Wilson TA, Karajannis MA, Harter DH (2014) Glioblastoma multiforme: state of the art and future therapeutics. Surg Neurol Int 5:64–7806.132138
5. Franceschi E, Bartolotti M, Brandes AA (2015) Bevacizumab in recurrent glioblastoma: Open issues. Future Oncol. https://doi.org/10.2217/fon.15.125
6. Miyajima M, Kusuhara H, Takahashi K et al (2013) Investigation of the effect of active efflux at the blood-brain barrier on the distribution of nonsteroidal aromatase inhibitors in the central nervous system. J Pharm Sci 102(9):3309–3319
7. Wijaya J, Fukuda Y, Schuetz JD (2017) Obstacles to brain tumor therapy: Key ABC transporters. Int J Mol Sci 18(12):https://doi.org/10.3390/ijms18122544
8. Kim SS, Harford JB, Pirollo KF, Chang EH (2015) Effective treatment of glioblastoma requires crossing the blood-brain barrier and targeting tumors including cancer stem cells: The promise of nanomedicine. Biochem Biophys Res Commun 468(3):485–489
9. Lonning PE, Geisler J, Bhatnager A (2003) Development of aromatase inhibitors and their pharmacologic profile. Am J Clin Oncol 26(4):S3–S8
10. Dave N, Sengaonkar V, Chow LML, Kendler A, LaSance K, Desai PB (2015) ATPS-13 Aromatase expression in high grade gliomas: a potential new target for therapy. Neurooncol 17(Suppl 5):v20–v21
11. Duenas Jimenez JM, Candanedo Arellano A, Santerre A et al (2014) Aromatase and estrogen receptor alpha mRNA expression

as prognostic biomarkers in patients with astrocytomas. J Neurooncol 119(2):275–284
12. Dave N, Gudelsky GA, Desai PB (2013) The pharmacokinetics of letrozole in brain and brain tumor in rats with orthotopically implanted C6 glioma, assessed using intracerebral microdialysis. Cancer Chemother Pharmacol 72(2):349–357
13. Dave N, Chow LM, Gudelsky GA, LaSance K, Qi X, Desai PB (2015) Preclinical pharmacological evaluation of letrozole as a novel treatment for gliomas. Mol Cancer Ther 14(4):857–864
14. Tivnan A, Heilinger T, Ramsey JM et al (2017) Anti-GD2-ch14.18/CHO coated nanoparticles mediate glioblastoma (GBM)-specific delivery of the aromatase inhibitor, letrozole, reducing proliferation, migration and chemoresistance in patient-derived GBM tumor cells. Oncotarget 8(10):16605–16620
15. Okada S, Vaeteewoottacharn K, Kariya R (2018) Establishment of a patient-derived tumor xenograft model and application for precision cancer medicine. Chem Pharm Bull (Tokyo) 66(3):225–230
16. Morton JJ, Bird G, Refaeli Y, Jimeno A (2016) Humanized Mouse Xenograft Models: Narrowing the Tumor-Microenvironment Gap. Cancer Res 76:6153–6158
17. Zhou Q, Facciponte J, Jin M, Shen Q, Lin Q (2014) Humanized NOD-SCID IL2rg−/− mice as a preclinical model for cancer research and its potential use for individualized cancer therapies. Cancer Lett 344:13–19
18. Apparaju SK, Gudelsky GA, Desai PB (2008) Pharmacokinetics of gemcitabine in tumor and non-tumor extracellular fluid of brain: an in vivo assessment in rats employing intracerebral microdialysis. Cancer Chemother Pharmacol 61(2):223–229
19. Paxinos G, Watson CR, Emson PC (1980) Ache-stained horizontal sections of the rat brain in stereotaxic coordinates. J Neurosci Methods 3(2):129–149
20. Gilant E, Kaza M, Szlagowska A, Serafin-Byczak K, Rudzki PJ (2012) Validated HPLC method for determination of temozolomide in human plasma. Acta Pol Pharm 69(6):1347–1355
21. Baker SD, Wirth M, Statkevich P et al (1999) Absorption, metabolism, and excretion of 14C-temozolomide following oral administration to patients with advanced cancer. Clin Cancer Res 5(2):309–317
22. Reyderman L, Statkevich P, Thonoor CM, Patrick J, Batra VK, Wirth M (2004) Disposition and pharmacokinetics of temozolomide in rat. Xenobiotica 34(5):487–500
23. Liu XD, Xie L, Zhong Y, Li CX (2000) Gender difference in letrozole pharmacokinetics in rats. Acta Pharmacol Sin 21(8):680–684
24. Buzdar AU, Robertson JF, Eiermann W, Nabholtz JM (2002) An overview of the pharmacology and pharmacokinetics of the newer generation aromatase inhibitors anastrozole, letrozole, and exemestane. Cancer 95(9):2006–2016
25. Buzdar AU (2003) Pharmacology and pharmacokinetics of the newer generation aromatase inhibitors. Clin Cancer Res 9(1 Pt 2):468S–468S72S
26. Wempe MF, Buchanan CM, Buchanan NL et al (2007) Pharmacokinetics of letrozole in male and female rats: Influence of complexation with hydroxybutenyl-beta cyclodextrin. J Pharm Pharmacol 59(6):795–802
27. Kalam A, Talegaonkar S, Vohora D (2017) Effects of raloxifene against letrozole-induced bone loss in chemically-induced model of menopause in mice. Mol Cell Endocrinol 440:34–43
28. Murai K, Yamazaki H, Nakagawa K, Kawai R, Kamataki T (2009) Deactivation of anti-cancer drug letrozole to a carbinol metabolite by polymorphic cytochrome P450 2A6 in human liver microsomes. Xenobiotica 39(11):795–802
29. Poca KS, Parente TE, Chagas LF et al (2017) Interstrain differences in the expression and activity of Cyp2a5 in the mouse liver. BMC Res Notes 10(1):125–017-2435-x
30. Zhou Q, Guo P, Kruh GD, Vicini P, Wang X, Gallo JM (2007) Predicting human tumor drug concentrations from a preclinical pharmacokinetic model of temozolomide brain disposition. Clin Cancer Res 13(14):4271–4279
31. Portnow J, Badie B, Chen M, Liu A, Blanchard S, Synold TW (2009) The neuropharmacokinetics of temozolomide in patients with resectable brain tumors: Potential implications for the current approach to chemoradiation. Clin Cancer Res 15(22):7092–7098
32. Ostermann S, Csajka C, Buclin T et al (2004) Plasma and cerebrospinal fluid population pharmacokinetics of temozolomide in malignant glioma patients. Clin Cancer Res 10(11):3728–3736
33. Agarwala SS, Kirkwood JM (2000) Temozolomide, a novel alkylating agent with activity in the central nervous system, may improve the treatment of advanced metastatic melanoma. Oncologist 5(2):144–151
34. Munoz JL, Walker ND, Scotto KW, Rameshwar P (2015) Temozolomide competes for P-glycoprotein and contributes to chemoresistance in glioblastoma cells. Cancer Lett 367(1):69–75
35. Schaich M, Kestel L, Pfirrmann M, Robel K, Illmer T, Kramer M, Dill C, Ehninger G, Schackert G, Krex D (2009) A MDR1 (ABCB1) gene single nucleotide polymorphism predicts outcome of temozolomide treatment in glioblastoma patients. Ann Oncol 20:175–181
36. de Gooijer MC, de Vries NA, Buckle T, Buil LCM, Beijnen JH, Boogerd W, van Tellingen O (2018) Improved Brain Penetration and Antitumor Efficacy of Temozolomide by Inhibition of ABCB1 and ABCG2. Neoplasia 20:710–720
37. Mahringer A, Fricker G (2010) BCRP at the blood-brain barrier: genomic regulation by 17beta-estradiol. Mol Pharm 7:1835–1847
38. Hartz AM, Mahringer A, Miller DS, Bauer B (2010) 17-beta-Estradiol: a powerful modulator of blood-brain barrier BCRP activity. J Cereb Blood Flow Metab 30:1742–1755
39. Kleinow KM, Hummelke GC, Zhang Y, Uppu P, Baillif C (2004) Inhibition of P-glycoprotein transport: a mechanism for endocrine disruption in the channel catfish? Mar Environ Res 58:205–208
40. Miller DS (2010) Regulation of P-glycoprotein and other ABC drug transporters at the blood-brain barrier. Trends Pharmacol Sci 31:246–254